**Proceedings of NTHC'00**
**34th ASME National Heat Transfer Conference**
**Pittsburgh, Pennsylvania, 20th - 22nd August, 2000**

# NHTC2000-12118

## NUMERICAL STUDY OF FORCED FLOW IN A BACK-STEP CHANNEL THROUGH POROUS LAYER

Edward C. Chan, M.A.Sc. Candidate
Lien Fue-Sang, Assistant Professor
M. Michael Yovanovich, Professor

Department of Mechanical Engineering
University of Waterloo, Waterloo, Ontario. N2L 3G1. Canada.

### ABSTRACT

In this work, we present a numerical solution for laminar and turbulent convective heat transfer in a backward-facing step channel through a porous insert. In addition to the Navier-Stokes equation for the fluid region, Brinkman-Forchheimer-extended Darcy's equation is introduced into the numerical solver to model the porous medium. In the turbulent flow scenarios, we use a two-equation $k$-$\varepsilon$ model with wall function for both the fluid region and the porous medium. The results obtained from the present study concur with existing benchmarks. For the turbulent flow results, it is observed that the amount of flow resistance offered by the porous insert is more heavily dependent on its width than the permeability.

### INTRODUCTION

The study of flow in porous media has received the attention of many inquiring minds for more than a century. Darcy [5] began the whole movement with his then-empirical relationship. Deviations due to form drag were addressed and rectified by Forchheimer [6], while Brinkman [4] extended Darcy's model for high-porosity media.

Following Wooding [20], who introduced convective effects into the porous media model, the governing equations somewhat resemble the Navier-Stokes equations. Beckermann et al. [3] were amongst the first to solve these equations, using conventional CFD techniques, in two dimensions. Their model could at least predict the trends with reasonable accuracy.

Vafai and Tien [17] noted a discrepancy in Wooding's equations. While the Darcy and Forchheimer terms were introduced based on a volume-averaged (seepage) velocity, the convective and Brinkman components were inspired by an instantaneous fluid (pore) velocity. They also made the appropriate adjustments for the two velocity scales, based on the porosity of the porous medium. Whitaker [19] later confirmed the observation in his formal and rigorous derivation of Darcy's law and Brinkman's extension from the Navier-Stokes equations alone.

Though turbulent modelling is still a subject of debate, it is clear, from works such as Ward [18] and MacDonald et. al. [12], that turbulence exists in porous media flow. Aside from its academic value, there are also many practical applications, from combustion to electronic cooling. Much of the research in this area is still in its infancy, however.

While there are many renowned turbulence models, only a handful account for the presence of porous media. This motivates the present investigation, allowing us to exploit opportunities for further improvement.

The turbulent model of interest is a $k$-$\varepsilon$ model based on the formulations by Lee and Howell [10] and Antohe and Lage [1]. It is then incorporated into the STREAM code applied to a turbulent flow over a backward-facing step [11]. Due to the lack of experimental data for a turbulent flow through a back-step channel with porous insert, validations were established through laminar test cases from Gartling [7], Le and Moin [9], and Martin et al. [13], Perić et al. [16], and Zhang and Zhao [21]. The trustworthiness of the present predictions is then inferred from these results.

### NOMENCLATURE

| | |
|---|---|
| $a$ | Width of porous insert [m] |
| $C_\mu$ | Constant for turbulent viscosity [] |

$C_{\varepsilon 1}$ Constant for turbulent dissipation rate production []
$C_{\varepsilon 2}$ Constant for turbulent dissipation rate destruction []
$Da_H$ Darcy number based on channel height []
$F$ Forchheimer number []
$H$ Height of channel [m]
$i, j$ Cartesian tensor indices[]
$k$ Turbulent kinetic energy [$m^2 \cdot s^{-2}$]
$P$ Fluid pressure [Pa]
$p$ Turbulent mean fluid pressure [Pa]
$p'$ Turbulent fluid pressure fluctuation [Pa]
$Pr$ Prandtl number []
$R_\alpha$ Ratio between effective and fluid $\alpha$ []
$R_\nu$ Ratio between effective and fluid $\nu$ []
$Re_H$ Reynolds number based on channel height []
$t$ Time [s]
$U$ Fluid / seepage velocity [$m \cdot s^{-1}$]
$u$ Turbulent mean fluid / seepage velocity [$m \cdot s^{-1}$]
$u'$ Turbulent fluid / seepage velocity fluctuation [$m \cdot s^{-1}$]
$x, y$ Cartesian co-ordinates [m]

**Greek Symbols**

$\varepsilon$ Dissipation rate of turbulent kinetic energy [$m^2 \cdot s^{-3}$]
$\phi$ Porous media porosity []
$\kappa$ Porous media permeability [$m^2$]
$\nu$ Fluid kinematic viscosity [$m^2 \cdot s^{-1}$]
$\nu_{eff}$ Effective kinematic viscosity [$m^2 \cdot s^{-1}$]
$\nu_T$ Eddy viscosity [$m^2 \cdot s^{-1}$]
$\rho$ Fluid density [$kg \cdot m^{-3}$]
$\sigma_k$ Turbulent Prandtl number for $k$ []
$\sigma_\varepsilon$ Turbulent Prandtl number for $\varepsilon$ []

## Flow Geometry

The problem under investigation consists of a channel with a backward-facing step at the entry region (see Figure 1.) The height of the back-step is half of that of the channel and it extends to two channel heights before it opens to the flow. The length of the full channel is long enough to let the flow become fully developed at the outlet. A porous insert immediately follows the back-step to provide some resistance to the flow.

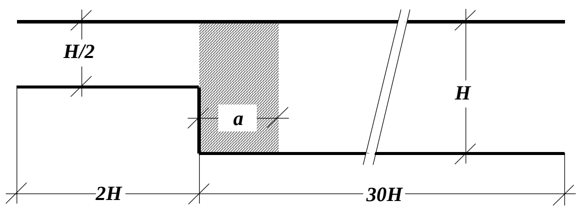


**Figure 1: Set-up for a backward-facing step channel with a porous insert after the step.**

Numerical results for such flow geometry, with and without the porous insert, are available from Gartling [7], Martin et al. [13], and Zhao and Zhang [21] for laminar flow. Perić et al. [16] also performed an extensive numerical study for the same case undergoing turbulence.

## Governing Equations – Laminar Flow

For completeness, below are the governing equations for incompressible flow in the fluid region:

$$\frac{\partial U_j}{\partial x_j} = 0 \tag{1}$$

$$\frac{\partial U_i}{\partial t} + U_j \frac{\partial U_i}{\partial x_j} = -\frac{1}{\rho}\frac{\partial P}{\partial x_i} + \nu \frac{\partial^2 U_i}{\partial x_j \partial x_j} \tag{2}$$

In the porous media region, however, we shall consider Darcy's Law [5], with Brinkman's [4] and Forchheimer's [6] extensions. Further, by analogy with the Navier-Stokes equation, convective terms are also added to the porous media flow equations.

It is noteworthy to mention that while the convective terms, as well as Brinkman's extension, are based on the fluid (pore) velocity alone, Darcy's Law and the Forchheimer term are derived using a volume-averaged (seepage) velocity. Vafai and Tien [17] proposed the relationship below between the two velocity scales:

$$U_{j,pore} = U_{j,seepage} / \phi \tag{3}$$

In order to maintain consistency with the fluid region, the governing equations in the porous media region are based on the *seepage* velocity which is denoted as $U_j$ (instead of $U_{j,seepage}$) from now on. Hence, we have the following governing equations for the porous media region:

$$\frac{\partial U_j}{\partial x_j} = 0 \tag{4}$$

$$\phi \frac{\partial U_i}{\partial t} + U_j \frac{\partial U_i}{\partial x_j} = -\frac{\phi^2}{\rho}\frac{\partial P}{\partial x_i} + \phi R_\nu \nu \frac{\partial^2 U_i}{\partial x_j \partial x_j} - \phi^2 \left( \frac{\nu}{\kappa} + \frac{F}{\sqrt{\kappa}} \sqrt{U_j U_j} \right) U_i \tag{5}$$

where $R_\nu = \nu_{eff} / \nu \approx 1$.

Though the presentation of the laminar flow equations is elementary, they form the basis for their turbulent counterparts.

## Governing Equations – Turbulence in Fluid Region

We will now consider the turbulence modelling in the fluid region. The $k$-$\varepsilon$ model is chosen here due to its low computational requirements. Let us first decompose the turbulent velocity and pressure fields as means and fluctuations, that is:

$$U_j = u_j + u'_j, \; P = p + p' \tag{6}$$

Next, we perform time-averaging on equations (1) and (2). This gives rise to the Reynolds stress terms, which are modelled using the concept of eddy viscosity. The resulting equations become:

$$\frac{\partial u_j}{\partial x_j}=0 \tag{7}$$

$$\frac{\partial u_i}{\partial t}+u_j\frac{\partial u_i}{\partial x_j}=-\frac{1}{\rho}\frac{\partial p}{\partial x_i}+\frac{\partial}{\partial x_j}\left[(\nu+\nu_T)\left(\frac{\partial u_i}{\partial x_j}+\frac{\partial u_j}{\partial x_i}\right)\right]-\frac{2}{3}\frac{\partial k}{\partial x_i} \tag{8}$$

where $\nu_T$ is known as the eddy viscosity. Meanwhile, $k$ represents the turbulent kinetic energy, and $\varepsilon$ is its dissipation rate. They are defined as follows:

$$\nu_T=C_\mu\frac{k^2}{\varepsilon},\quad k=\frac{\overline{u_i'u_i'}}{2},\quad \varepsilon=\nu\overline{\frac{\partial u_i'}{\partial x_j}\frac{\partial u_i'}{\partial x_j}} \tag{9}$$

Subsequently, we require transport equations for $k$ and $\varepsilon$ to close the problem, which can be derived from equations (2) and (8). Through appropriate modelling, the equations become:

$$\frac{\partial k}{\partial t}+u_j\frac{\partial k}{\partial x_j}=\frac{\partial}{\partial x_j}\left[\left(\nu+\frac{\nu_T}{\sigma_k}\right)\frac{\partial k}{\partial x_j}\right]+\nu_T\frac{\partial u_i}{\partial x_j}\left(\frac{\partial u_i}{\partial x_j}+\frac{\partial u_j}{\partial x_i}\right)-\varepsilon \tag{10}$$

$$\begin{aligned}\frac{\partial \varepsilon}{\partial t}+u_j\frac{\partial \varepsilon}{\partial x_j}=\frac{\partial}{\partial x_j}\left[\left(\nu+\frac{\nu_T}{\sigma_\varepsilon}\right)\frac{\partial \varepsilon}{\partial x_j}\right]+\\ C_{\varepsilon 1}\frac{\varepsilon}{k}\nu_T\frac{\partial u_i}{\partial x_j}\left(\frac{\partial u_i}{\partial x_j}+\frac{\partial u_j}{\partial x_i}\right)-C_{\varepsilon 2}\frac{\varepsilon^2}{k}\end{aligned} \tag{11}$$

with the single-value constants below, as proposed by Launder and Spalding [8]:

$$C_\mu=0.09,\ C_{\varepsilon 1}=1.44,\ C_{\varepsilon 2}=1.92,\ \sigma_k=1.0,\ \sigma_\varepsilon=1.3 \tag{12}$$

## Governing Equations – Turbulence in Porous Region

The main issue surrounding turbulence modelling in porous media flow is the local time-averaging process. While Whitaker [19] derived Darcy's Law and Brinkman's extension for any representative elementary volume, which infers the possibility of local time-averaging, the same cannot be said for the Forchheimer term, as it represents form drag [2]. In particular, the treatment of the $\sqrt{U_jU_j}$ term in the Forchheimer term is the subject of interest.

Antohe and Lage [1] perform a local time average on the Forchheimer term itself, which later gives rise to its inconclusive contribution to the $k$ and $\varepsilon$ equations. Lee and Howell [10], on the other hand, suggested using only the mean velocity in the square-root term, that is, $\sqrt{U_jU_j}=\sqrt{u_ju_j}$.

Owed to its empirical origin, it is uncertain whether or not the time-average process has been implicitly performed on the Forchheimer's term. Hence, the Lee and Howell's approach was adopted. This results in the following governing equations for turbulent flow in porous media:

$$\frac{\partial u_j}{\partial x_j}=0 \tag{13}$$

$$\begin{aligned}\phi\frac{\partial u_i}{\partial t}+u_j\frac{\partial u_i}{\partial x_j}=-\frac{\phi^2}{\rho}\frac{\partial p}{\partial x_i}+\phi\frac{\partial}{\partial x_j}\left[(R_\nu\nu+\nu_T)\left(\frac{\partial u_i}{\partial x_j}+\frac{\partial u_j}{\partial x_i}\right)\right]-\\ \frac{2}{3}\frac{\partial k}{\partial x_i}-\phi^2\left(\frac{\nu}{\kappa}+\frac{F}{\sqrt{\kappa}}\sqrt{u_ju_j}\right)u_i\end{aligned} \tag{14}$$

$$\begin{aligned}\phi\frac{\partial k}{\partial t}+u_j\frac{\partial k}{\partial x_j}=\phi\frac{\partial}{\partial x_j}\left[\left(\nu+\frac{\nu_T}{\sigma_k}\right)\frac{\partial k}{\partial x_j}\right]+\nu_T\frac{\partial u_i}{\partial x_j}\left(\frac{\partial u_i}{\partial x_j}+\frac{\partial u_j}{\partial x_i}\right)-R_\nu\varepsilon-\\ 2\phi^2\left(\frac{\nu}{\kappa}+\frac{F}{\sqrt{\kappa}}\sqrt{u_ju_j}\right)k\end{aligned} \tag{15}$$

$$\begin{aligned}\phi\frac{\partial \varepsilon}{\partial t}+u_j\frac{\partial \varepsilon}{\partial x_j}=\phi\frac{\partial}{\partial x_j}\left[\left(\nu+\frac{\nu_T}{\sigma_\varepsilon}\right)\frac{\partial \varepsilon}{\partial x_j}\right]+C_{\varepsilon 1}\frac{\varepsilon}{k}\nu_T\frac{\partial u_i}{\partial x_j}\left(\frac{\partial u_i}{\partial x_j}+\frac{\partial u_j}{\partial x_i}\right)-\\ R_\nu C_{\varepsilon 2}\frac{\varepsilon^2}{k}-2\phi^2\left(\frac{\nu}{\kappa}+\frac{F}{\sqrt{\kappa}}\sqrt{u_ju_j}\right)\varepsilon\end{aligned} \tag{16}$$

Antohe and Lage [1] argued that the pore size ultimately restrains the size of the largest eddy within the porous matrix. Assuming that the porous material is isotropic, this favours the hypothesis of isotropic turbulence. This strengthens the support in using the eddy viscosity model.

## Initial, Boundary, & Interface Conditions

The velocity distribution at the channel inlet is chosen such that the entrance average velocity is 1. Taking into account the back-step, the following inlet profiles is valid between $y = H/2$ and $y = H$:

$$u_{inlet}=\begin{cases}24\left(1-\dfrac{y}{H}\right)\left(\dfrac{y}{H}-\dfrac{1}{2}\right) & ;\ \text{Laminar}\\ \dfrac{8}{7}\left(1-4\left|\dfrac{y}{H}-\dfrac{3}{4}\right|\right)^{1/7} & ;\ \text{Turbulent}\end{cases}\quad ;\ y=\left(\frac{H}{2},H\right) \tag{17}$$

For the fluid flow, the no-slip boundary conditions are imposed in both the channel walls and the step. Finally, the flow at the interface between the fluid and the porous region must be continuous. The presence of the Brinkman's extension and the convective terms in the porous media equation eliminates the need for imposing an explicit interface condition in this case [3, 14], since these terms also guarantee continuity of the interfacial shear stress.

## Numerical Solution Method

The present flow solver is based on the STREAM code [11], designed for a general non-orthogonal grid with the SIMPLE algorithm [15] for pressure correction. Modifications were made to accommodate turbulence and porous media models.

Wall functions were used to approximate the near-wall behaviour at high Reynolds number, whilst macroscopic conservation principles are observed at the channel outlet. The second-order linear upwind difference (LUDS) scheme was used for approximating the advection. The computational domain for the channel is covered by $100 \times 60$ control volumes. The numerical solution is deemed convergent when the magnitude of the accumulated residual goes below $10^{-3}$.

## Laminar Flow Results

There are three benchmarks available for the back step flow: Le and Moin [9], Gartling [7], and Zhang and Zhao [21]. The first two cases only include fluid flow, and the last one includes effects of a porous insert at various thickness and permeability. The following parameters were used throughout: $Re = 800$, $\phi = 0.97$, $F = 0.1$, $H = 1$.

First, we consider the reattachment length without the porous insert at different Reynolds numbers ($\mathrm{Re}_H = \bar{u}H/\nu$). The results are in excellent agreement with the results of Le and Moin [9] (Figure 2). Note that Le and Moin used a Reynolds number based on the maximum velocity (i.e., $u_{max} = 3\bar{u}/2$) and the appropriate adjustment has been made here.

Next, let us concentrate on the case where $Re_H = 800$, where detailed results may be obtained from Gartling [7]. From Figure 3 below, the present results predict the general flow patterns very well. Gartling, however, reported that the reattachment length of the lower-wall bubble is $6.1H$, whilst it is only $5.65H$ in the present study, which agrees well with Le and Moin's prediction [9]. Nevertheless, a horizontal velocity profile at $x = 7H$ and $x = 15H$ showed very good agreement between the two studies.

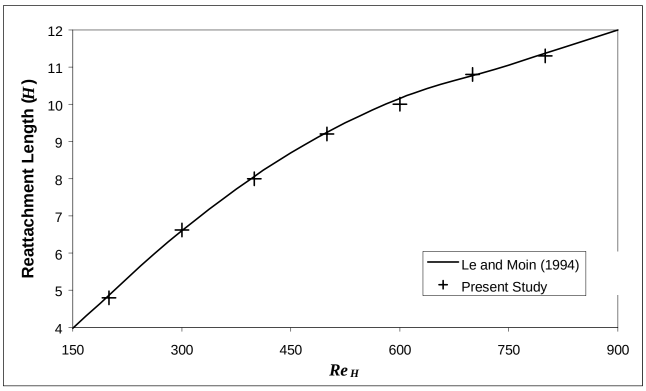


**Figure 2: Reattachment length as a function of Reynolds number for laminar flows.**

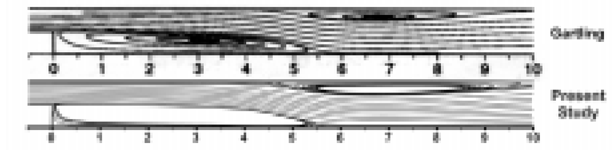


**Figure 3: Comparison of streamtraces for $Re_H$ = 800 between Gartling, top, and present study, bottom.**

To conclude the validation, we have also compared our results with those of Zhang and Zhao [21]. From Martin et al [13], it is of practical interest to optimise the width of the porous insert in order to reduce or even eliminate the re-circulation zone. This, in turn, optimises between improved heat transfer characteristics and head loss. In this case, however, the re-circulation zone serves as a benchmark for the present flow solver. Presented here are only cases where the re-circulation zone is prominently featured, all at $Re_H$ = 800. The present results, shown in Figure 4, Figure 5 and Figure 6, are in good agreement with the benchmarks.

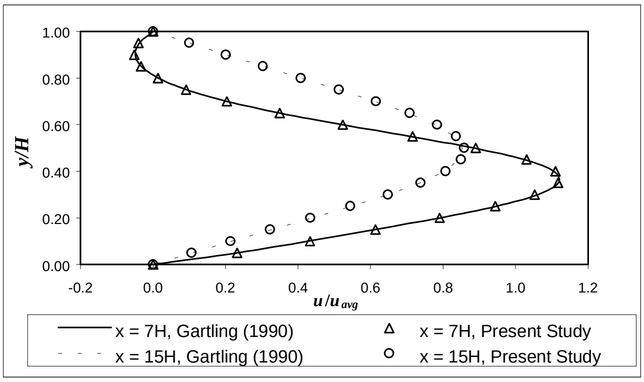


**Figure 4: Comparison of streamwise velocity at $x/H$ = 7 and $x/H$ = 15 with Gartling.**

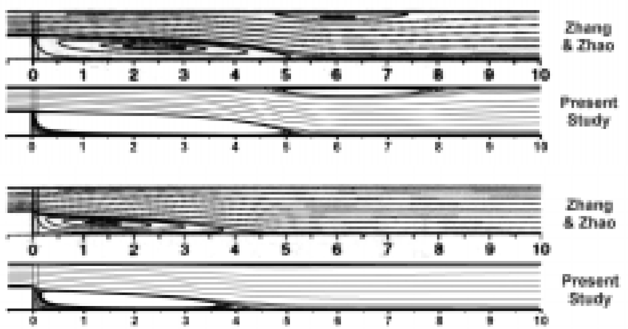


**Figure 5: Comparison of streamtraces for $Da_H = 10^{-2}$ (top) and $10^{-3}$ (bottom) between Zhang and Zhao and present study for porous insert width $a = 0.1\ H$.**

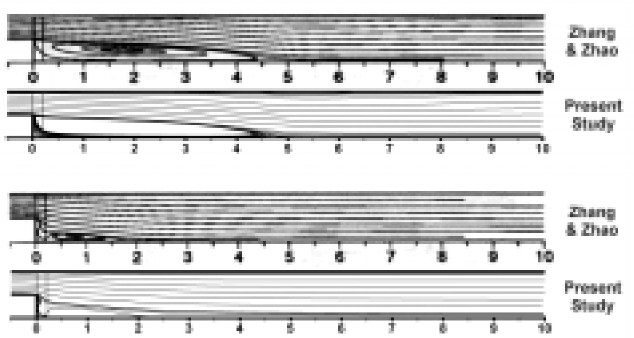


**Figure 6: Comparison of streamtraces for $Da_H$ = $10^{-2}$ (top) and $10^{-3}$ (bottom) between Zhang and Zhao and present study for porous insert width *a* = 0.2 *H*.**

## Turbulent Flow Results

For turbulent flow, we set $Re_H$ to 25 000 while the other parameters remain unchanged. For validation, we obtain a converged solution without the porous insert and compare the results with Perić et al. [16], who also employed the high-Reynolds number turbulent model with wall functions for their flow calculation. They have reported a grid-independent re-attachment length of 3.76 *H*. Our programme, on the other hand, reported 3.6 *H*, under the same flow conditions. Given the present grid distribution, both results are in very good agreement. Figure 7 shows the corresponding streamtraces.

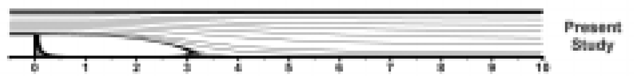


**Figure 7: Streamtraces under a fully turbulent flow regime with no porous insert. The re-attachment length is 3.6 *H*.**

Afterwards, we reinstate the porous insert and execute the four cases, as we have previously, under a turbulent flow regime. The results are illustrated in Figure 8 and Figure 9. It is noteworthy to mention that, for cases where the porous insert is thin (*a* = 0.1*H*), the re-attachment length changes very little, regardless the permeability of the porous insert. The influence of the permeability becomes more apparent when the porous insert becomes much thicker. The effects, however, are not still as far-reaching as in the laminar case.

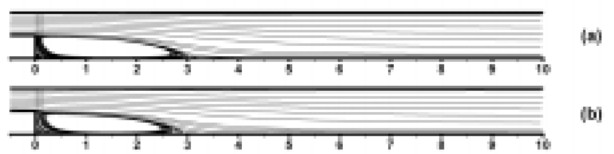


**Figure 8: Streamtraces under a fully turbulent flow regime at $Da_H$ = (a) $10^{-2}$ and (b) $10^{-3}$ with a porous insert width of *a* = 0.1 *H*.**

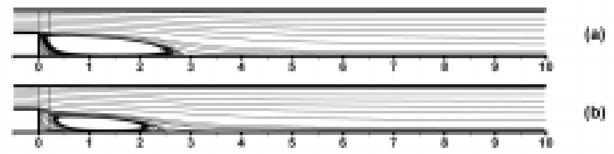


**Figure 9: Streamtraces under a fully turbulent flow regime at $Da_H$ = (a) $10^{-2}$ and (b) $10^{-3}$ with a porous insert width of *a* = 0.2 *H*.**

## Summary and Conclusion

A turbulent model using wall function has been developed to account for flow through a porous medium. The coupled equations are successively solved using the SIMPLE algorithm. The results are then compared with existing cases for laminar and turbulent flow.

The laminar flow results agree extremely well with all the presently cited cases. As expected, the porous insert successfully dampens the flow, greatly shrinking the re-circulation zone. The effect is both immediate and notable, either in the insert's permeability or thickness. When the flow is fully turbulent, however, the amount of resistance offered by the insert is more heavily dependent on the thickness than permeability. In particular, the porous insert has virtually no influence on the flow if it is thin and highly permeable.

Future work will be focused on deriving the same governing equations for the low-Reynolds number turbulence model, as well as more extensive testing on a variety of materials. Heat transfer results are currently being produced.


## ACKNOWLEDGEMENTS

I would like to extend my gratitude to the Natural Sciences and Engineering Research Council for its financial support. Also, many thanks go to Dr. José L. Lage, from whom I drew insights and inspiration while undertaking this project. Finally, I wish to take this opportunity to express my admiration to Hr. Martin Eibl, who has painstakingly located Forchheimer's original paper [6] from across the Atlantic. It has been a great pleasure studying such a classic work.


## REFERENCES


1. Antohe, B.V., and Lage, J.L.. "A General Two-Equation Macroscopic Turbulence model for Incompressible Flow in Porous Media." *International Journal of Heat and Mass Transfer*, **40**, pp 3013-3024, 1997.
2. Bear, J.. *Dynamics of Fluids in Porous Media*, American Elsevier, 1972.
3. Beckermann, C., Viskanta, R., and Ramadhyani, S.. "Natural Convection in Vertical Enclosures Containing

Simultaneously Fluid and Porous Layers." *Journal of Fluid Mechanics*, **186**, pp 257-284, 1987.

4. Brinkman, H.C.. "Calculations of the Flow of Heterogeneous Mixture through Porous Media." *Applied Science Research*, **2**, pp 81-86, 1948.
5. Darcy, H.. *Les Fontaines Publiques de la Ville de Dijon*, Dalmont, Paris, 1856.
6. Forchheimer, P.. "Wasserbewegung durch Boden." (Part 2) *Zeitschrift des Vereines Deutscher Ingenieure*, **45**, pp 1781-1788, 1901.
7. Gartling, D.K.. "A Test Problem for Outflow Boundary Conditions – Flow over a Backward-Facing Step." *International Journal for Numerical Methods in Fluids*, **11**, pp 953-967, 1990.
8. Launder, B.E., and Spalding, D.B.. "The Numerical computation of Turbulent Flows." *Computer Methods in Applied Mechanics and Engineering*, **3**, pp 269-289, 1974.
9. Le, H., and Moin, P.. *Direct Numerical simulation of turbulent Flow over a Backward-Facing Step*, Report TF-58, Stanford University, 1994.
10. Lee, K., and Howell, J.R.. "Forced Convective and Radiative Transfer within a Highly Porous Layer Exposed to a Turbulent External Flow Field." *Proceedings of the ASME-JSME Thermal Engineering Joint Conference*, **2**, pp 377-386, 1987.
11. Lien, F.-S., and Leschziner, M.A.. "Assessment of Turbulence-Transport Models including Non-Linear RNG Eddy-Viscosity Formulation and Second-Moment Closure for Flow over a Backward-Facing Step." *Computer and Fluids*, **23**, pp 983-1004, 1994.
12. MacDonald, I.F., El-Sayed, M.S., Mow, K., and Dullien, F.A.L.. "Flow through Porous Media – Ergun Equation Revisited." *Industrial Engineering and Chemical Fundamentals*, **18**, pp 199-208, 1979.
13. Martin, A.R., Saltiel, C., and Shyy, W.. "Heat Transfer Enhancement with Porous Inserts in Recirculating Flows." ASME Journal of Heat Transfer, **120**, pp 258-467, 1998.
14. Nield, D.A., and Bejan, A.. *Convection in Porous Media*, Springer-Verlag, 1992.
15. Patankar, S.. *Numerical Heat Transfer and Fluid Flow*, Hemisphere, 1980.
16. Perić, M., Rüger, M., and Scheuerer, G.. "A Finite Volume Multigrid Method for Calculating Turbulent Flows." Seventh Symposium on Turbulent Shear Flows, pp 7.3.1 – 7.3.6, 21st-23rd August, 1989.
17. Vafai, K., and Tien, C.-L.. "Boundary and Inertia Effects on Flow and Heat Transfer in Porous Media." *International Journal of Heat and Mass Transfer*, **24**, pp 195-203, 1981.
18. Ward, J.C.. "Turbulent Flow in Porous Media." *Proceeding of the ASCE Journal of Hydraulics*, **90**, HY5, pp 1-12, 1964.
19. Whitaker, S.. "Flow in Porous Media I: A Theoretical Derivation of Darcy's Law." *Transport in Porous Media*, **1**, pp 3-25, 1986.
20. Wooding, R.A. "Steady State Free Thermal Convection of Liquid in a Saturated Permeable Medium." Journal of Fluid Mechanics, **2**, pp 273-285, 1957.
21. Zhang, B., and Zhao, Y.. "Numerical simulations of Fluid Flow and Convection Heat Transfer through Fluid/Porous Layers." *AIAA 33rd Thermophysics Conference*, AIAA 99-3627, 1999.

 